APPLICATION OF THE METHOD OF INTEGRAL RELATIONS TO SUPERSONIC NONEQUILIBRIUM FLOW PAST WEDGES AND CONES

by Jerry C. South, Jr.

Langley Research Center
Langley Station, Hampton, Va.

NATIONAL AERONAUTICS AND SPACE ADMINISTRATION • WASHINGTON, D. C. • AUGUST 1964

APPLICATION OF THE METHOD OF INTEGRAL RELATIONS TO SUPERSONIC NONEQUILIBRIUM FLOW PAST WEDGES AND CONES

By Jerry C. South, Jr.

Langley Research Center
Langley Station, Hampton, Va.

NATIONAL AERONAUTICS AND SPACE ADMINISTRATION

For sale by the Office of Technical Services, Department of Commerce,
Washington, D.C. 20230 -- Price $1.00

APPLICATION OF THE METHOD OF INTEGRAL RELATIONS TO SUPERSONIC NONEQUILIBRIUM FLOW PAST WEDGES AND CONES

By Jerry C. South, Jr.
Langley Research Center

SUMMARY

The method of integral relations is used to calculate supersonic nonequilibrium flow past wedges and circular cones at zero incidence. Vibrational relaxation in a pure diatomic gas is considered so that the results can be compared with existing calculations using the method of characteristics. The approach taken is similar to that followed previously in ideal-gas problems, except that the isentropic law cannot be used and the vibrational rate equation is included. The governing equations are converted to approximate systems of ordinary differential equations which are solved as initial-value problems on a high-speed digital computer. Alternate procedures are discussed which point out certain features of general importance.

Numerical results are presented to illustrate the convergence and accuracy of the method in predicting the distributions of flow variables during the approach to equilibrium. The calculations are performed through the third approximation for the wedge and through the second approximation for the cone.

INTRODUCTION

The method of integral relations (ref. 1) is a numerical analysis technique for solving the nonlinear equations of gas dynamics. Specifically designed for high-speed computing, the method has been shown to be useful and versatile in a variety of problems. Most applications have been in mixed flows, such as the sonic flow past ellipses and ellipsoids (ref. 2) and the supersonic blunt-body problem (refs. 3 to 9). Other important applications have been made to conical flows without axial symmetry (ref. 10) and to the viscous boundary layer (ref. 11).

In the aforementioned works the gas was considered to be ideal; thus, an obvious step would seem to be the extension of this method to include real-gas effects in hypersonic flow problems. There do not appear to be any obstacles to such an extension in the case of equilibrium thermodynamics. The entropy is still conserved along the streamlines and, therefore, the stream function can

be used advantageously (refs. 3 and 6). Usually the variations of equilibrium flow properties across the shock layer are no more nonlinear than are those in ideal-gas cases. In nonequilibrium flows, however, there are some difficulties: the isentropic law is not valid and cannot be used; chemical and vibrational rate equations must be included; and shock-layer profiles can be highly nonlinear. This last difficulty is particularly important to a basic feature of the method: the assumption of interpolation polynomials for certain groupings of the flow variables. The nonlinear profiles may be poorly approximated by low-degree polynomials and might considerably retard the convergence of the method. On the other hand, the integral relations effect a "smoothing" of profile irregularities (ref. 11); thus it seems possible that some significant results might be obtained in low-degree approximations.

Two applications of the integral relations to nonequilibrium flow calculations have recently appeared. Shih et al. (ref. 12) used the first approximation to calculate hypersonic flow of a five-component (N_2,O_2,N,O, and NO) dissociating gas past a sphere. Some of the different procedures necessary for nonequilibrium calculations, as compared with previous ideal-gas work (refs. 3 to 9), were emphasized, particularly in regard to the starting conditions at the axis of symmetry.

South (ref. 13) applied the integral relations to supersonic, nonequilibrium flow past wedges and cones, where the molecular vibrations are relaxing. As in reference 12, only the first approximation was considered, but the results for shock-wave shape and surface pressure distribution compared favorably with calculations based on the method of characteristics (supplied by R. Sedney and N. Gerber of the Ballistic Research Laboratories, Aberdeen Proving Ground). In reference 13 the vibrational relaxation time was assumed to be constant throughout the wedge or cone shock layer to eliminate dependence on experimental results for the relaxation time. The computational program was later modified to account for a pressure- and temperature-dependent relaxation time, and the first approximation results were found to be adversely affected. Similar unpublished calculations made at the Langley Research Center using the Lighthill-Freeman dissociating gas model showed that the first approximation was inadequate. It appears that in many problems approximations higher than the first may be needed.

In the present paper, the work of reference 13 is extended to higher approximations in a straightforward manner. The prime objective is to observe the resulting gains in overall accuracy, with emphasis on certain important features of the method of integral relations that have not been evident previously.

SYMBOLS

c_p frozen-flow specific heat at constant pressure

E vibrational energy

E_{eq} equilibrium vibrational energy

F	nonhomogeneous functions in equations (1) to (4), used in equations (14) to (19)
G	functions differentiated with respect to y in equations (1) to (4), used in equations (14) to (19)
j	0 or 1 for a wedge or a cone, respectively
M	frozen-flow Mach number, $\frac{V}{\sqrt{\gamma p/\rho}}$
N	order of approximation (number of strips)
p	pressure
Q	functions differentiated with respect to x in equations (1) to (4), used in equations (14) to (19)
R	gas constant
r	radial coordinate normal to cone axis
T	temperature
u,v	velocity component in x- and y-direction, respectively
V	total velocity, $\sqrt{u^2 + v^2}$
x,y	coordinate along and normal to body surface, respectively
Δx	integration step size
β	shock-wave angle
γ	ratio of frozen-flow specific heats
δ	shock-layer thickness in y-direction
ϵ	vibrational driving force, $\frac{E_{eq} - E}{\tau}$
Θ_v	characteristic vibrational temperature
θ	wedge or cone half-angle
λ	shock-layer included angle, $\beta - \theta$
ρ	density

τ vibrational relaxation time

ψ stream function

Subscripts:

∞ free-stream quantity

i 1,2,3,4 (refers to continuity, x-momentum, y-momentum, and rate equations, respectively)

0 surface quantity; see definition of subscript k

k 0,1,. . .,N-1,δ (denotes a particular strip boundary as labeled in fig. 2)

δ shock-wave quantity; see definition of subscript k

Primed quantities are dimensional; unprimed quantities are dimensionless, as shown after equation (6).

Barred quantities are corrected surface flow variables.

PROBLEM DESCRIPTION

The physical problem to be studied is the steady supersonic flow of a pure diatomic gas past symmetric wedges and right circular cones. The flow is inviscid and the only dissipative mechanism is the relaxation process of the molecular vibrations. This is then the same problem studied in references 14 and 15 by using the method of characteristics. There are several reasons why this model is well suited to the objectives of the present study. The governing equations are relatively simple in form, yet the physical problem is highly nonlinear and exhibits many of the important features of more complex nonequilibrium flows. The added difficulties which arise in the blunt-body problem (refs. 3 to 9 and 12), such as unknown initial conditions and multiple singular points, are not encountered here. This is a great advantage in numerical calculations, particularly in higher approximations. Finally, it seems worthwhile to point out that radiation heating problems (refs. 16 and 17) have caused a renewed interest in pointed configurations, such as the wedge or the cone, for the design of hypersonic vehicles.

Basic Equations

The flow geometry and coordinate system are illustrated in figure 1 for a cone. A body-oriented coordinate system, with x and y the coordinates along and normal to the body surface, is used so that the X-axis is inclined to the stream direction by the angle θ and coincides with the wedge or cone surface. The wedge or cone tip lies at the point (0,0). The basic equations are as follows (ref. 13):

Continuity:

$$\frac{\partial}{\partial x}\left(\rho u r^j\right) + \frac{\partial}{\partial y}\left(\rho v r^j\right) = 0 \tag{1}$$

x-momentum:

$$\frac{\partial}{\partial x}\left[\left(p + \rho u^2\right) r^j\right] + \frac{\partial}{\partial y}\left(\rho u v r^j\right) - j p \sin\theta = 0 \tag{2}$$

y-momentum:

$$\frac{\partial}{\partial x}\left(\rho u v r^j\right) + \frac{\partial}{\partial y}\left[\left(p + \rho v^2\right) r^j\right] - j p \cos\theta = 0 \tag{3}$$

Vibrational rate:

$$\frac{\partial}{\partial x}\left(\rho u E r^j\right) + \frac{\partial}{\partial y}\left(\rho v E r^j\right) - \rho \epsilon r^j = 0 \tag{4}$$

Energy:

$$T + E + \frac{\gamma - 1}{2} M_\infty^2 \left(u^2 + v^2\right) = 1 + \frac{\gamma - 1}{2} M_\infty^2 \tag{5}$$

State:

$$\gamma M_\infty^2 p = \rho T \tag{6}$$

where $j = 0$ or 1 for a wedge or cone, respectively, and $r = x \sin\theta + y \cos\theta$. The variables and coordinates have been nondimensionalized as follows:

$$u,v = \frac{u',v'}{V_\infty'} \qquad p = \frac{p'}{\rho_\infty' V_\infty'^2} \qquad \rho = \frac{\rho'}{\rho_\infty'}$$

$$T = \frac{T'}{T_\infty'} \qquad E = \frac{E'}{c_p' T_\infty'} \qquad x,y = \frac{x',y'}{L'}$$

The primes denote dimensional quantities. The length scale L' is taken to be $V_\infty' \tau'(0,0)$, where $\tau'(0,0)$ is the vibrational relaxation time on the surface at the wedge or cone tip. It is assumed, as in references 14 and 15, that

$$p'\tau' \propto \exp\left(C'/T'\right)^{1/3} \tag{7}$$

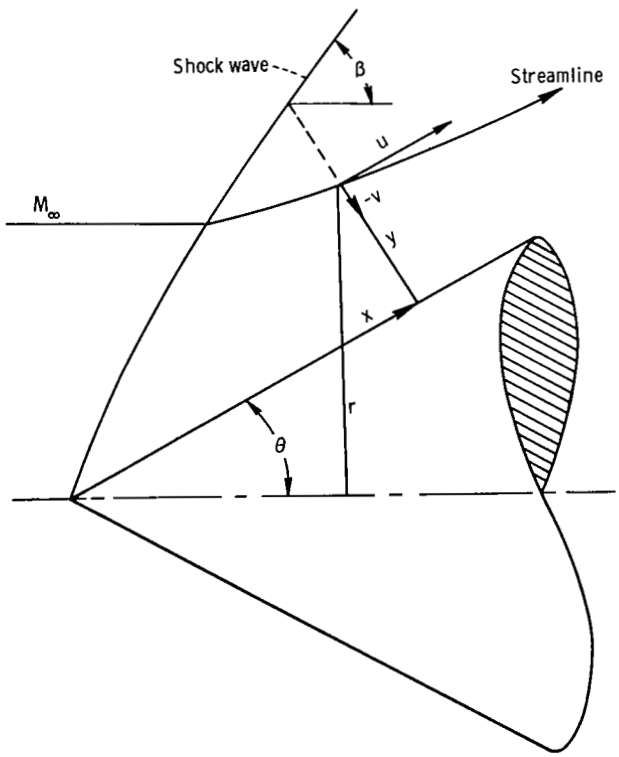

Figure 1.- Flow geometry and coordinate system for a cone.

where the constant C' is determined from experimental data. The vibrational "driving force" ϵ appearing in equation (4) is (as in refs. 14 and 15)

$$\epsilon = \frac{E_{eq} - E}{\tau} \tag{8}$$

where $\tau = \tau'/\tau'(0,0)$ and E_{eq} is the vibrational energy that the flow would have locally if it were in equilibrium at temperature T and is taken to be

$$E_{eq} = \frac{2}{7}\Theta_v\left[\exp\left(\frac{\Theta_v}{T}\right) - 1\right]^{-1} \tag{9}$$

The factor $2/7$ is the ratio R'/c_p' for an ideal diatomic gas ($\gamma = 7/5$).

Boundary Conditions

It is assumed that the molecular vibrations are frozen across the shock wave and that $E_\infty = 0$; then, at the shock curve, or $y = \delta(x)$,

$$E(x,\delta) = E_\delta(x) = 0 \tag{10}$$

The ideal-gas shock-wave relations apply and the other variables can be determined as algebraic functions of M_∞, θ, and the shock-wave angle $\beta(x)$. The necessary relations are listed in appendix A.

The location of the shock curve is determined by

$$\frac{d\delta}{dx} = \tan\lambda \tag{11}$$

where $\lambda = \beta - \theta$, and the shock wave is attached at the body tip so that

$$\delta(0) = 0 \tag{12}$$

The wedge or cone surface is a streamline; thus

$$v(x,0) = v_0(x) = 0 \tag{13}$$

APPROXIMATE SYSTEMS

The method of integral relations provides a logical procedure for converting equations (1) to (4) to approximate systems of ordinary differential equations, which are readily adaptable to electronic digital computing. The conversion procedure for the present problem is the same as that used in previous ideal-gas, mixed-flow studies (refs. 1 and 3). The first approximation was derived in detail in reference 13, and higher approximations used herein are straightforward extensions of that work.

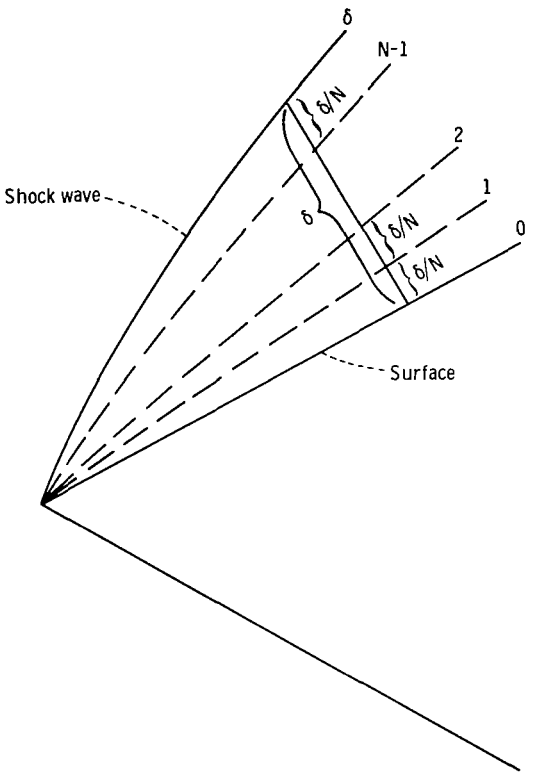

Figure 2.- Nth-strip arrangement.

Equations (1) to (4) are in the divergence form - that is,

$$\frac{\partial Q_i}{\partial x} + \frac{\partial G_i}{\partial y} - F_i = 0 \qquad (i = 1,2,3,4) \qquad (14)$$

where the appropriate functions Q_i, G_i, and F_i can be seen by inspection of equations (1) to (4). In the Nth approximation the region of flow between the shock wave and body surface is divided into N equal strips, arranged as in figure 2. Each of equations (14) is integrated from the surface ($y = 0$) to the boundary of each strip. The result is (for the present problem) 4N integral relations, as follows:

$$\frac{d}{dx}\int_0^{y_k} Q_i \, dy - Q_{i,k}\frac{dy_k}{dx} + G_{i,k} - G_{i,0} - \int_0^{y_k} F_i \, dy = 0 \qquad (15)$$

$$(i = 1,2,3,4)$$
$$(k = 1,2,\ldots,N-1,\delta)$$

To evaluate the unknown integrals, Nth-degree interpolation polynomials in y are assumed for the functions Q_i and F_i; for example,

$$Q_i = \sum_{n=0}^{N} q_{i,n} y^n \qquad (16)$$

where the coefficients $q_{i,n}$ depend linearly on the x-dependent functions $Q_{i,k}$. An approximate system of 4N ordinary differential equations is finally obtained, where x is the independent variable.

Corresponding to the general form indicated by equations (14), the first three approximations (N = 1,2,3) can be written as follows:

N = 1: (i = 1,2,3,4)

$$\delta \frac{dQ_{i,0}}{dx} + \delta \frac{dQ_{i,\delta}}{dx} + \left(Q_{i,0} - Q_{i,\delta}\right)\frac{d\delta}{dx} - 2\left(G_{i,0} - G_{i,\delta}\right) - \delta\left(F_{i,0} + F_{i,\delta}\right) = 0 \tag{17}$$

N = 2: (i = 1,2,3,4)

$$\delta \frac{dQ_{i,0}}{dx} - \delta \frac{dQ_{i,\delta}}{dx} + \left(Q_{i,0} - 4Q_{i,1} + 3Q_{i,\delta}\right)\frac{d\delta}{dx}$$
$$- 4\left(G_{i,0} - 2G_{i,1} + G_{i,\delta}\right) - \delta\left(F_{i,0} - F_{i,\delta}\right) = 0 \tag{18a}$$

$$2\delta \frac{dQ_{i,1}}{dx} + \delta \frac{dQ_{i,\delta}}{dx} + 4\left(Q_{i,1} - Q_{i,\delta}\right)\frac{d\delta}{dx}$$
$$- G_{i,0} - 4G_{i,1} + 5G_{i,\delta} - \delta\left(2F_{i,1} + F_{i,\delta}\right) = 0 \tag{18b}$$

N = 3: (i = 1,2,3,4)

$$2\delta \frac{dQ_{i,0}}{dx} + 2\delta \frac{dQ_{i,\delta}}{dx} + \left(2Q_{i,0} - 9Q_{i,1} + 18Q_{i,2} - 11Q_{i,\delta}\right)\frac{d\delta}{dx}$$
$$- 13G_{i,0} + 27G_{i,1} - 27G_{i,2} + 13G_{i,\delta} - 2\delta\left(F_{i,0} + F_{i,\delta}\right) = 0 \tag{19a}$$

$$3\delta \frac{dQ_{i,1}}{dx} - \delta \frac{dQ_{i,\delta}}{dx} + 6\left(Q_{i,1} - 2Q_{i,2} + Q_{i,\delta}\right)\frac{d\delta}{dx}$$
$$- 2G_{i,0} - 9G_{i,1} + 18G_{i,2} - 7G_{i,\delta} - \delta\left(3F_{i,1} - F_{i,\delta}\right) = 0 \tag{19b}$$

$$6\delta \frac{dQ_{i,2}}{dx} + 2\delta \frac{dQ_{i,\delta}}{dx} + 3\left(Q_{i,1} + 4Q_{i,2} - 5Q_{i,\delta}\right)\frac{d\delta}{dx}$$
$$+ G_{i,0} - 9G_{i,1} - 9G_{i,2} + 17G_{i,\delta} - 2\delta\left(3F_{i,2} + F_{i,\delta}\right) = 0 \tag{19c}$$

The second subscript refers to a particular strip boundary, as indicated in figure 2. Since the shock-wave functions $Q_{i,\delta}$ are functions of β (and r_δ when $j = 1$), equations (17) to (19) were manipulated so that derivatives of $Q_{i,\delta}$ and only one other function, $Q_{i,k}$ $(k = 0,1,\ldots,N-1)$, appear in each equation. This form is algebraically convenient because $d\beta/dx$ can be obtained easily from the single equation containing $dQ_{3,0}/dx$ and $dQ_{3,\delta}/dx$ (e.g., eq. (17), (18a), or (19a)) by noting that $Q_{3,0} = \rho_0 u_0 v_0 = 0$ for all values of x. The algebra required to obtain the remaining derivatives of u_k, v_k, etc., is considerably simplified. Further details are given in appendix B, where the final computational equations are derived for the second approximation, $N = 2$.

It should be noted that in the approximate systems the functions $Q_{i,k}$ contain the factor $r_k{}^j$. If the derivatives of $r_k{}^j$ are expanded and the equations are then divided by $r_0{}^j$, the resulting differential equations for the cone are very similar to those for the wedge, with some added terms (for example, see ref. 13 for $N = 1$ and appendix B for $N = 2$).

Tip Solution

The condition that the shock wave is attached, or $\delta(0) = 0$, causes the coefficients of the derivatives to vanish at the tip of the wedge or cone. If a regular solution exists, it is necessary that the remaining terms also vanish at $x = 0$. This condition yields $4N$ algebraic equations in the $5N$ unknowns: β; $u_0,\ldots,u_{N-1}$; $v_1,\ldots,v_{N-1}$; $p_0,\ldots,p_{N-1}$; $\rho_0,\ldots,\rho_{N-1}$; and $E_0,\ldots,E_{N-1}$ $\left(u_\delta,\ v_\delta,\text{ etc., are considered to be functions of } \beta \text{ through the shock-wave relations, with } M_\infty \text{ and } \theta \text{ specified}\right)$. Eliminating T_k between equations (5) and (6) on each strip boundary gives N additional equations; this step completes the initial solution.

The N algebraic equations which correspond to the rate equation $(i = 4)$ together with equation (10) yield $E_k = 0$; that is, the flow is frozen throughout the shock layer at the wedge or cone tip. The remaining equations yield the exact solution for frozen flow over a wedge when $j = 0$; that is, $u_k = u_\delta$, $v_k = v_\delta = 0$, $p_k = p_\delta$, etc. When $j = 1$, an approximate solution for frozen flow past a cone is obtained, and this solution is especially interesting.

In the classical problem of supersonic frozen or equilibrium flow past an axisymmetric cone, similarity considerations show that the shock wave is straight and that flow properties are constant along rays emanating from the tip. Application of the same considerations to the approximate systems for the continuity and momentum equations is straightforward, since all strip boundaries are straight rays when the shock is straight. Discarding the x-derivatives of the flow variables along the strip boundaries yields the same solution for all values of x as the limit solution $(x \to 0)$ mentioned previously. This

particular application of the integral relations was also pointed out by Chushkin and Shchennikov (ref. 10). It is worth noting that where the exact classical solutions result from a boundary-value problem for nonlinear ordinary differential equations, the integral relations yield nonlinear algebraic equations which are solved by trial and error. Some results of these solutions are shown in figure 3, wherein the first (N = 1) and second (N = 2) approximations for frozen flow over a cone are compared with the exact solution (ref. 18). In reference 19 it was shown that the first approximation agrees well with the exact solution (ref. 20) for full equilibrium airflow over a cone.

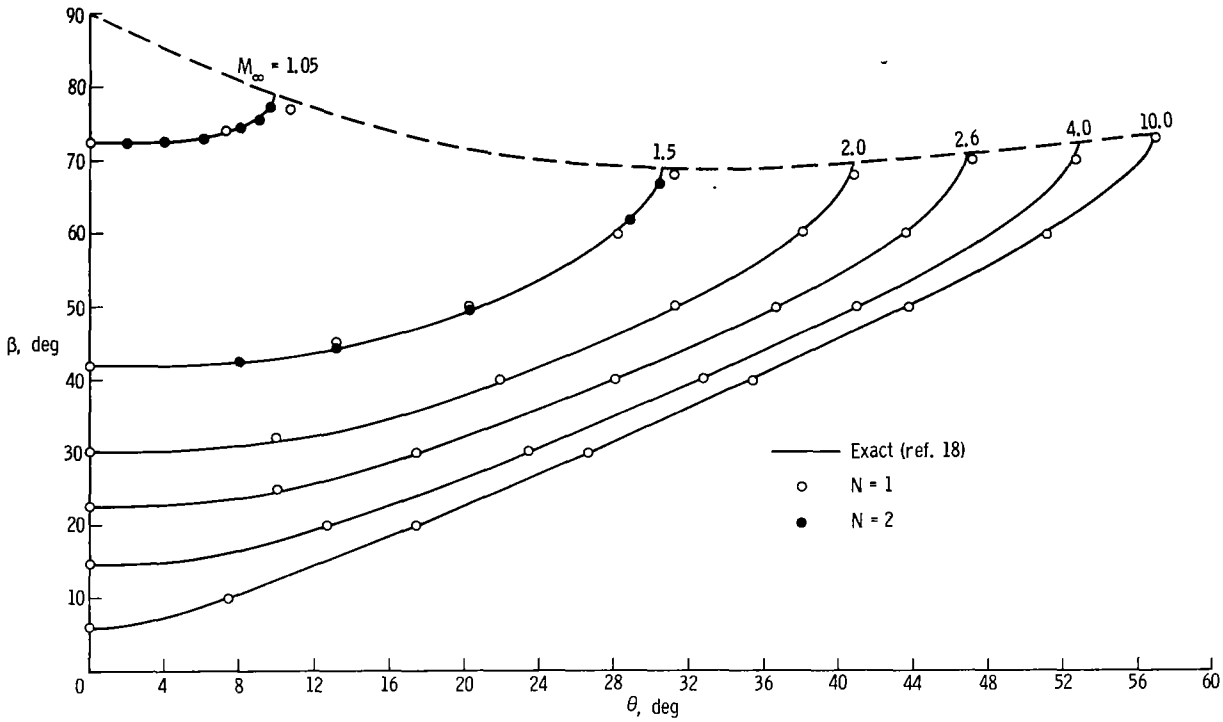

Figure 3.- Shock-wave angle as a function of cone half-angle for frozen flow.

For the present problem in which the entire shock layer is supersonic,[1] the initial values of the flow variables are completely determined by the approximate systems and the shock-wave relations. Since the original partial differential equations are of hyperbolic type (ref. 22), the integral relations properly form an initial-value problem. (In the blunt-body problem, with subsonic flow in the nose region and supersonic flow on the afterbody, the partial differential equations are of mixed (elliptic and hyperbolic) type; and the integral relations thus form a boundary-value problem (refs. 3 to 8).)

[1]At a given value of $M_\infty > 1$, there exists a limited region of wedge or cone angles which are smaller than the detachment angle, yet subsonic flow occurs in the shock layer (ref. 21, p. 683). This situation is excluded in the present formulation.

The initial derivatives at $x = 0$ can be evaluated by differentiating the approximate systems once more and taking the limit $(x \to 0)$. The initial derivatives so obtained for the wedge are exact in all approximations. This result is not surprising, since the frozen-flow variables at the wedge tip are constant in the interval $0 \leqq y \leqq \delta$ (and $\delta \to 0$); thus, the interpolation polynomials assumed for ρu, ρuv, etc., are exact at $x = 0$. The wedge initial derivatives on any strip boundary are derived in appendix C.

The present method also yields linear algebraic equations for the cone tip derivatives. The approximate expressions are more lengthy than those for the wedge and are not given herein; they are given in reference 13 for $N = 1$. The exact solution for the cone tip derivatives can be obtained in a manner similar to that for the wedge (see appendix C) by solving a boundary-value problem for linear ordinary differential equations. The integration must be performed numerically, however, since the variable coefficients of the differential equations depend on the nonlinear conical-flow solution. The present approximate calculations for the cone tip derivatives for $N = 2$ were found to be in excellent agreement with exact numerical solutions recently obtained by R. Sedney and N. Gerber of the Ballistic Research Laboratories, Aberdeen Proving Ground.

Nonconvergence of the Rate Equation

At large distances from the wedge or cone tip, it can be intuitively reasoned that throughout most of the shock layer the flow variables should approach their equilibrium values - that is, those values which arise from assuming zero relaxation time behind the shock wave. For a finite relaxation time, there are three zones which appear in the flow: (1) a relaxation zone just behind the shock wave, (2) an equilibrium zone between the shock wave and surface, and (3) an entropy layer adjacent to the surface (ref. 14). Far from the tip, the equilibrium zone (2) will occupy most of the shock layer so that by comparison the relative thicknesses of zones (1) and (3) appear to be negligibly thin. Zones (1) and (3) do not actually disappear, however, and this feature causes difficulty in any calculation scheme. For example, the flow variables at the surface, excepting the pressure, do not reach the same equilibrium values as in zone (2), and the flow variables at the shock are always frozen even at $x = \infty$. The profiles of the flow variables across the shock layer thus approach jump discontinuities at both the shock wave and surface as $x \to \infty$.

In the present method, this difficulty is evidenced in the approximate systems for the rate equation ($i = 4$). The vibrational driving forces ϵ_k along the strip boundaries appear in the $F_{4,k}$ terms of the approximate systems. Each of those driving forces should tend to zero as x increases, with the exception of the shock-wave driving force ϵ_δ. The boundary condition at the shock wave (eq. (10)) gives for all values of x

$$\epsilon_\delta = \frac{E_{eq,\delta}}{\tau_\delta} > 0 \tag{20}$$

A closer examination of the approximate systems reveals that the coefficients of the physical-variable derivatives contain the factor δr_k^j which is of the order x^{1+j} for large values of x. In the approximate rate equations, the $\delta F_{4,k}$ terms $\left(= \delta r_k^j \rho_k \epsilon_k\right)$ are also of the order x^{1+j}. Then equating the coefficients of x^{1+j} (that is, comparing the dominant terms for large values of x) leads to the following conclusion: the physical derivatives along the strip boundaries can decay to zero as x increases only if ϵ_k $(k \neq \delta)$ approach unrealistic nonzero values to counter the always-positive contribution of ϵ_δ. This effect is the most severe in the surface rate equation (e.g., eq. (17), (18a), or (19a)) since, as $x \to \infty$,

$$\epsilon_0 \to \pm \left(\frac{r_\delta}{r_0}\right)^j \frac{\rho_\delta}{\rho_0} \epsilon_\delta \tag{21}$$

or

$$E_0 \to E_{eq,0} \pm \left(\frac{r_\delta}{r_0}\right)^j \frac{\rho_\delta \tau_0}{\rho_0 \tau_\delta} E_{eq,\delta} \tag{22}$$

where the plus sign corresponds to $N = 1$ and 3 and the minus sign corresponds to $N = 2$. Equation (22) predicts alternating "overshoots" (+) and "undershoots" (-) of about equal magnitude in the asymptotic value for E_0. The problem is less severe at the interior strip boundaries, since the $F_{4,k}$ terms $(k \neq 0,\delta)$ receive more weight than the $F_{4,\delta}$ terms. For example, in equations (19b) and (19c) $F_{4,1}$ and $F_{4,2}$ are weighted three times as much as $F_{4,\delta}$.

NUMERICAL RESULTS

Three different numerical cases are presented to illustrate the accuracy and convergence of the method. The conditions for each case herein correspond exactly to the conditions for the calculated examples reported in references 14 and 15. Thus, the results obtained by using the method of integral relations can be directly compared with those obtained by the method of characteristics. For all cases the free-stream temperature is 300° K and the gas is pure nitrogen ($\Theta_v = 11.12$). The constant $C = C'/T_\infty'$ used in the expression for the vibrational relaxation time (eq. (7)) was obtained from the authors of references 14 and 15. The numerical cases are as follows:

Case I - Wedge: $M_\infty = 6$, $\theta = 40.02°$, $C = 0.4655 \times 10^4$

Case II - Cone: $M_\infty = 12$, $\theta = 46.39°$, $C = 1.0137 \times 10^4$

Case III - Cone: $M_\infty = 10$, $\theta = 53.82°$, $C = 1.0137 \times 10^4$

Hyperbolic Stability Criterion

In reference 13 only the first approximation was considered, and no numerical stability problems were encountered in cases I and II. In case III the initial Mach number (based on the frozen speed of sound) on the cone surface M_0 was about 1.08, and all attempts at integration away from the tip failed. It was believed that the instability was caused by the fact that $M_0 = 1$ is a natural singular point of the system. The higher approximations were later discovered to be unstable not only in case III but also in cases I and II ($M_0 \approx 1.4$ and 1.7, respectively). The problem was finally resolved by applying a hyperbolic stability criterion, as follows: Consider the two-strip ($N = 2$) calculation for flow past a wedge, schematically illustrated in figure 4. Three data points along the surface normal are computed at each integration step: at the shock, at the middle line, and on the surface. The left-running (C^+) and the right-running (C^-) Mach line characteristics emanating from the three points intersect downstream approximately as shown at some point ($x + \Delta x$). For a stable calculation, the local step size must not be greater than that given by the approximate characteristic mesh. For the purpose of obtaining an approximate criterion, it is assumed that all the streamlines are parallel to the surface and the local Mach number is equal to M_0. The geometry then gives for $N = 2$

$$\Delta x \leq \frac{\delta}{4}\left(M_0^2 - 1\right)^{1/2} \qquad (23)$$

By the same reasoning it can be shown that for any value of N

$$\Delta x \leq \frac{\delta}{2N}\left(M_0^2 - 1\right)^{1/2} \qquad (24)$$

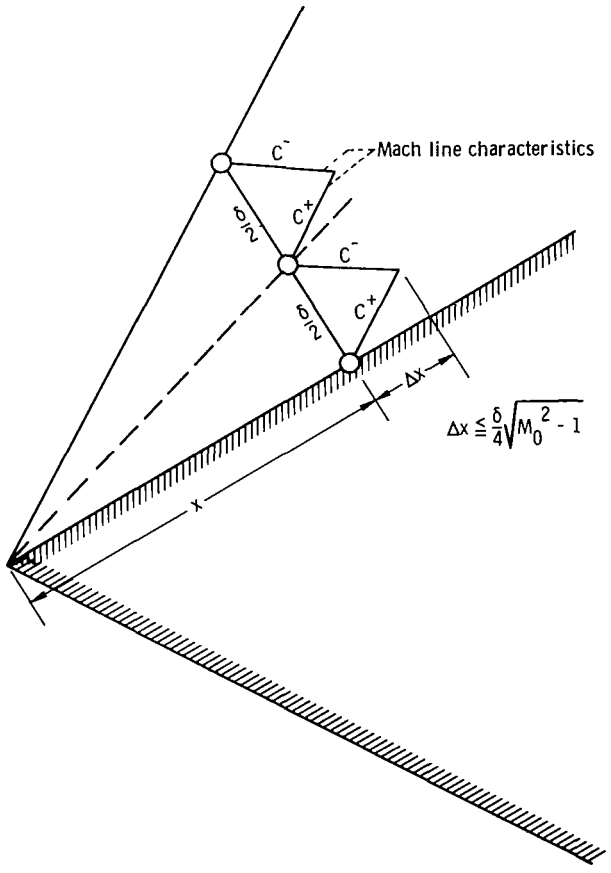

Figure 4.- Approximate hyperbolic stability criterion ($N = 2$).

Since the criterion given by equation (24) is approximate, it is usually necessary to use some fraction of that criterion to insure success. The criterion cannot be applied at the initial step since $\delta(0) = 0$; therefore, a single linear step is taken at $x = 0$, and the criterion is applied thereafter.

In figure 5 the calculated surface pressure distribution near the wedge tip is shown for case I and $N = 2$. The solid curve is an unstable calculation using

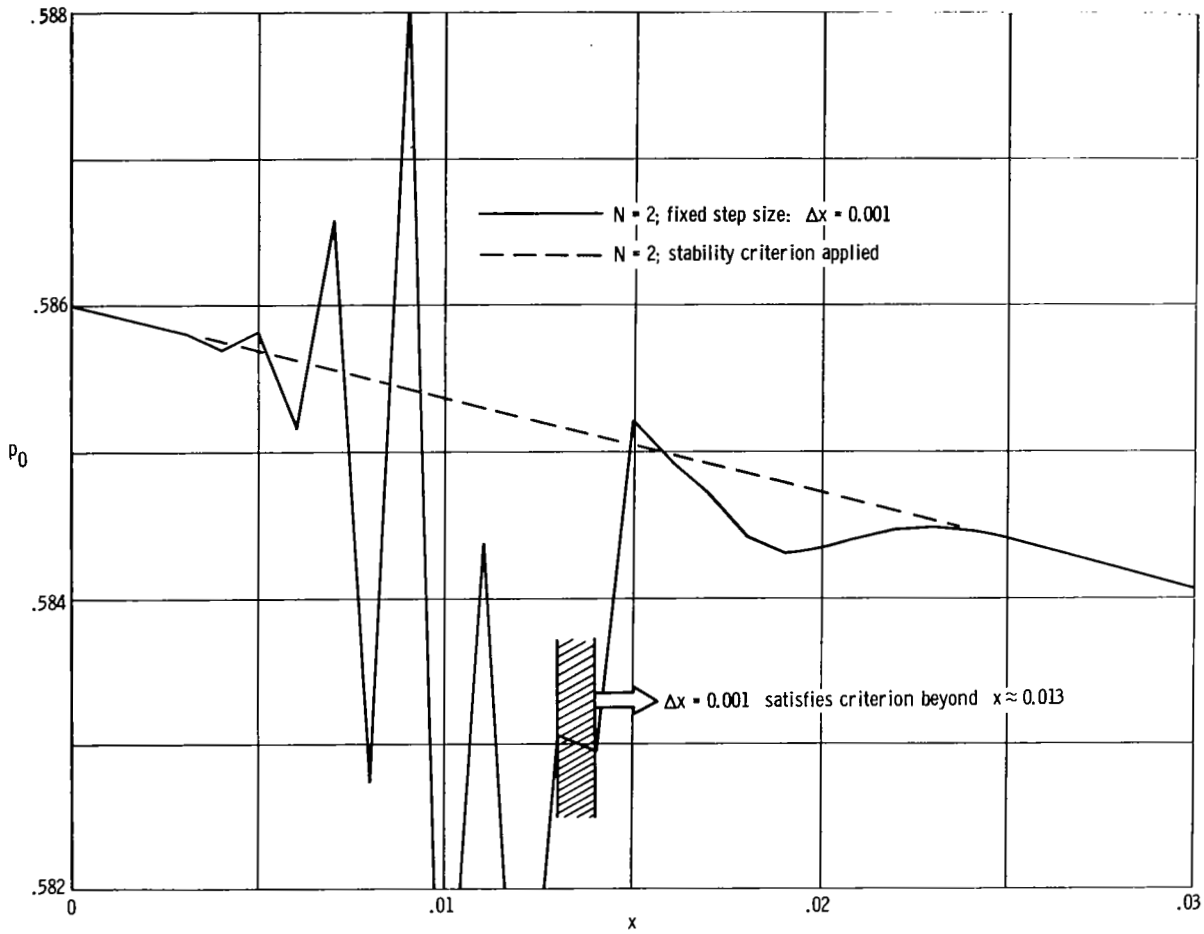

Figure 5.- Effect of hyperbolic stability criterion. Case I.

a first-order Euler integration procedure with a fixed step size Δx of 0.001. For the initial conditions of this case, that step size satisfies the $N = 2$ stability criterion when $x > 0.013$. Note that the solution stabilized at that point. The dashed curve is also a first-order Euler integration with an initial step size Δx of 0.001, but the $N = 2$ stability criterion was applied at every successive step, and the results are stable.

The stability criterion was included in the computational program used in reference 13, and case III was successfully integrated. In reference 13 cases I and II were integrated (for $N = 1$) without the stability criterion because the automatic step-sizing built into the Runge-Kutta integration scheme was able to satisfy the $N = 1$ criterion within the first few steps.

Pressure Distribution and Shock-Wave Shape

Calculations for the wedge (case I) were performed for $N = 1$, 2, and 3. For the cone, the algebraic solutions which give the initial values and derivatives are far more tedious in higher approximations than for the wedge; therefore, cone calculations for $N = 3$ were not attempted.

The results for surface pressure distribution $p_0(x)$ and shock-wave shape $\beta(x)$ are shown in figures 6 to 8, together with the characteristics calculations

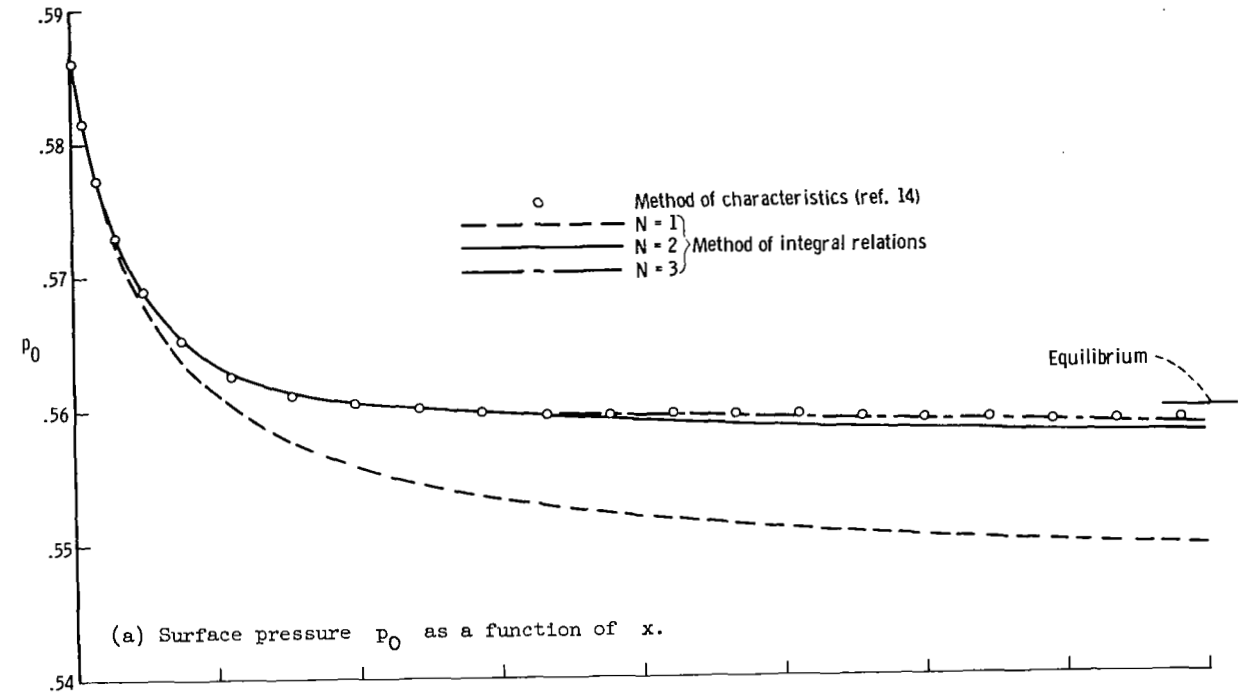

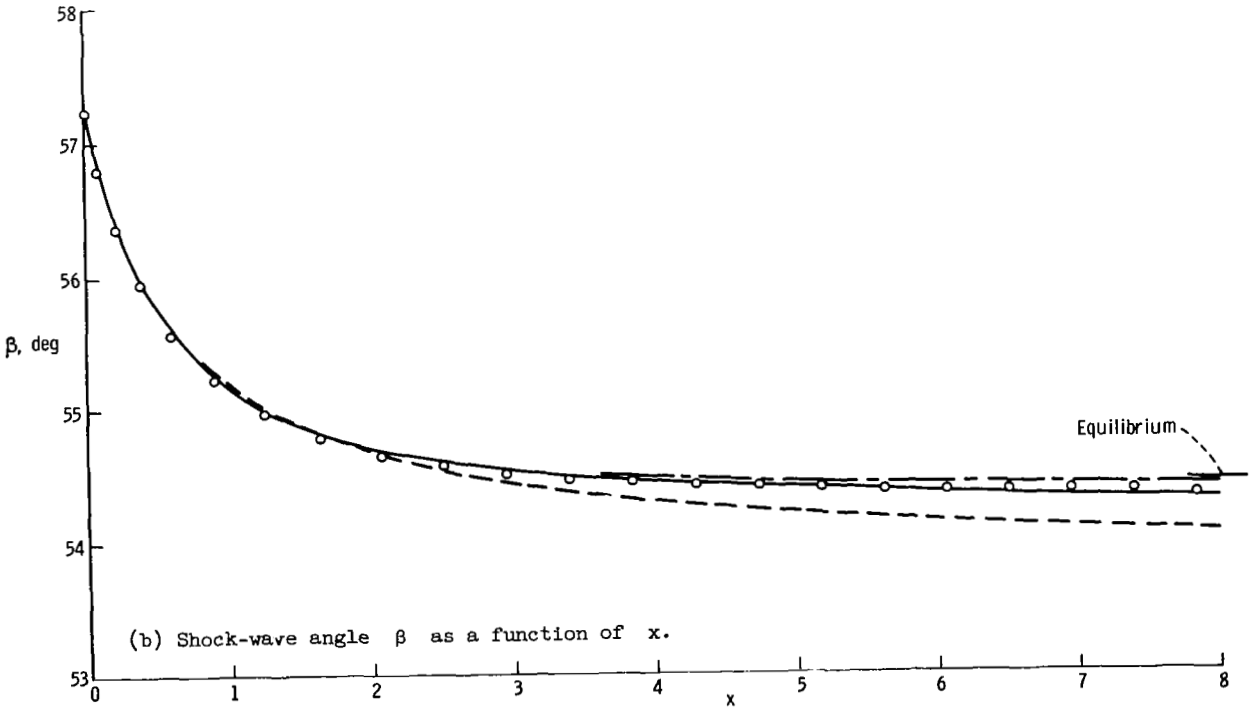

Figure 6.- Pressure distribution and shock-wave shape for a wedge. Case I.

of references 14 and 15. The short horizontal line at the right of each figure indicates the level for vibrational equilibrium ($\tau' = 0$) flow. For the three

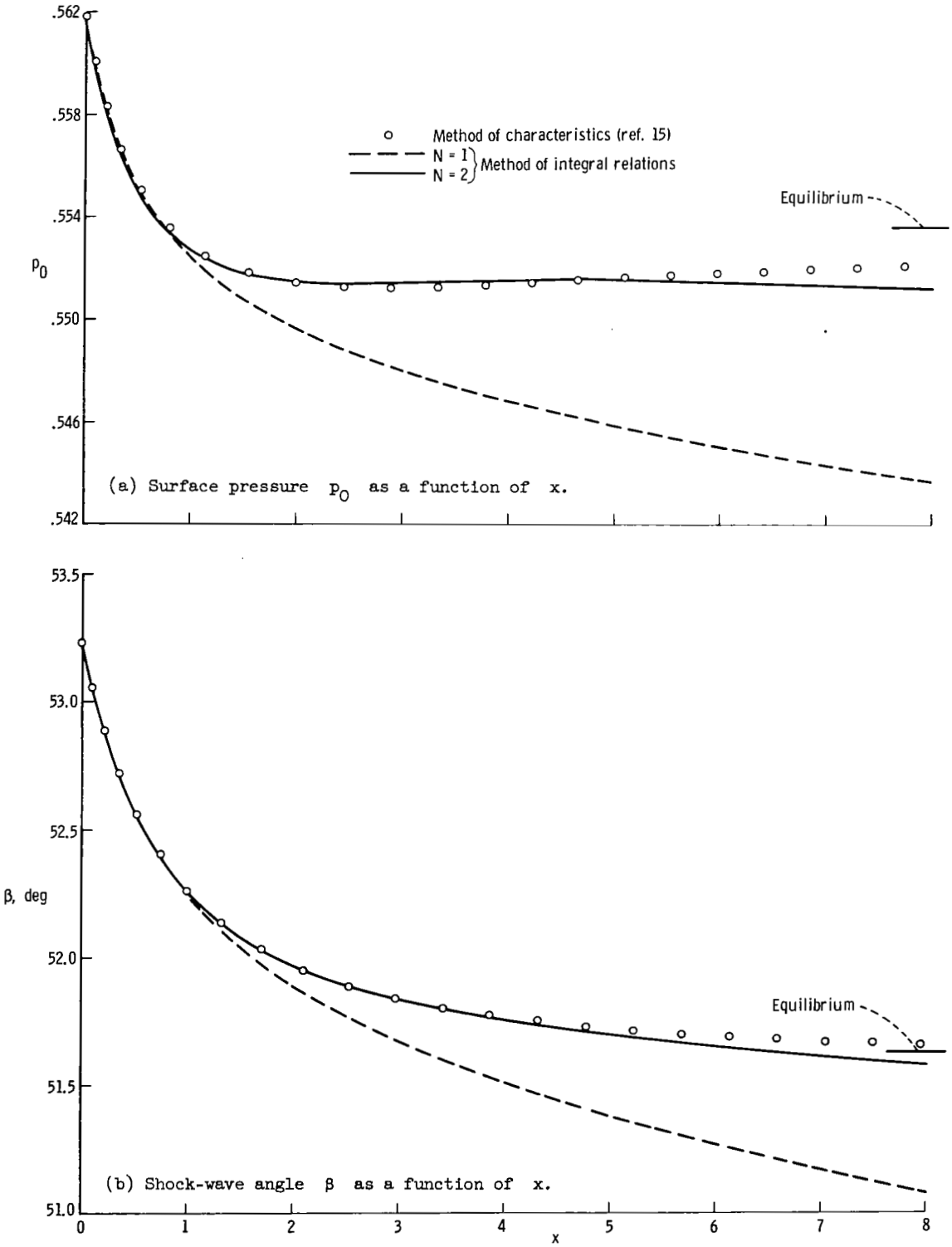

Figure 7.- Pressure distribution and shock-wave shape for a cone. Case II.

cases most of the approach to equilibrium is adequately described by $N = 2$, and the accuracy of $N = 2$ is considerably improved compared with that of $N = 1$. The nonconvergence of the surface vibrational energy, explained previously, has a detrimental effect on the asymptotic values of all the variables, but the effect decreases as N increases. Figure 9 illustrates the surface vibrational-energy distribution $E_0(x)$ for case I. The erroneous overshoots and undershoots mentioned earlier are clearly evident.

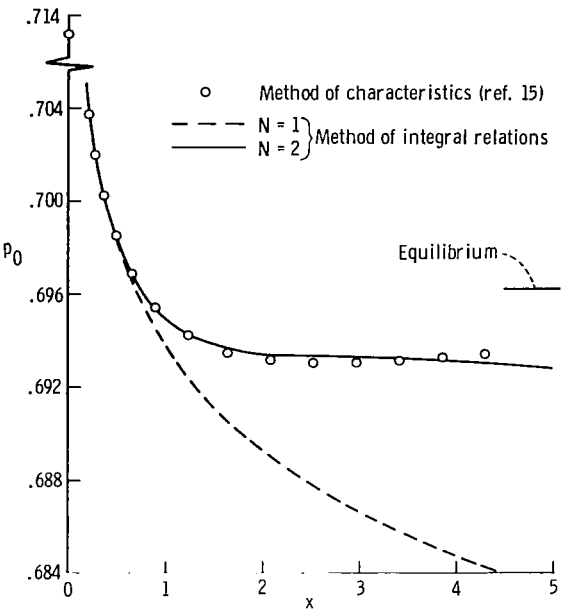

Figure 8.- Surface pressure distribution for a cone. Case III.

Improvements for Certain Surface Variables

In reference 13 it was pointed out that the approximate differential equations are not equivalent to the correct x-momentum and streamline rate equations at the surface - that is,

$$\frac{du_0}{dx} = -\frac{1}{\rho_0 u_0}\frac{dp_0}{dx} \tag{25}$$

and

$$\frac{dE_0}{dx} = \frac{\epsilon_0}{u_0} \tag{26}$$

The discrepancy occurs in all approximations largely because the integral relations must account for $v(\partial u/\partial y)$ and $v(\partial E/\partial y)$ throughout the shock layer. As was shown in reference 13, equations (25) and (26) can be used together with equations (5) and (6) to give improved distributions $\bar{u}_0(x)$, $\bar{E}_0(x)$, $\bar{T}_0(x)$, and $\bar{\rho}_0(x)$, consistent with the pressures $p_0(x)$ obtained from the approximate equations. The corrected surface vibrational-energy distribution $\bar{E}_0(x)$ is shown in figure 9, and the improvement is excellent. A note of caution is necessary, however: the corrected surface variables $\bar{u}_0$, $\bar{E}_0$, etc., are obtained in addition to the corresponding original variables u_0, E_0, etc. It is tempting to replace the two approximate differential equations for u_0 and E_0 by the exact equations (25) and (26). Such a "hybrid" procedure was used in the nonequilibrium blunt-body study of reference 12, and it was tried in the early stages of the present work. In the present application, the hybrid procedure always produced an unstable system. Unbounded oscillations of the derivatives

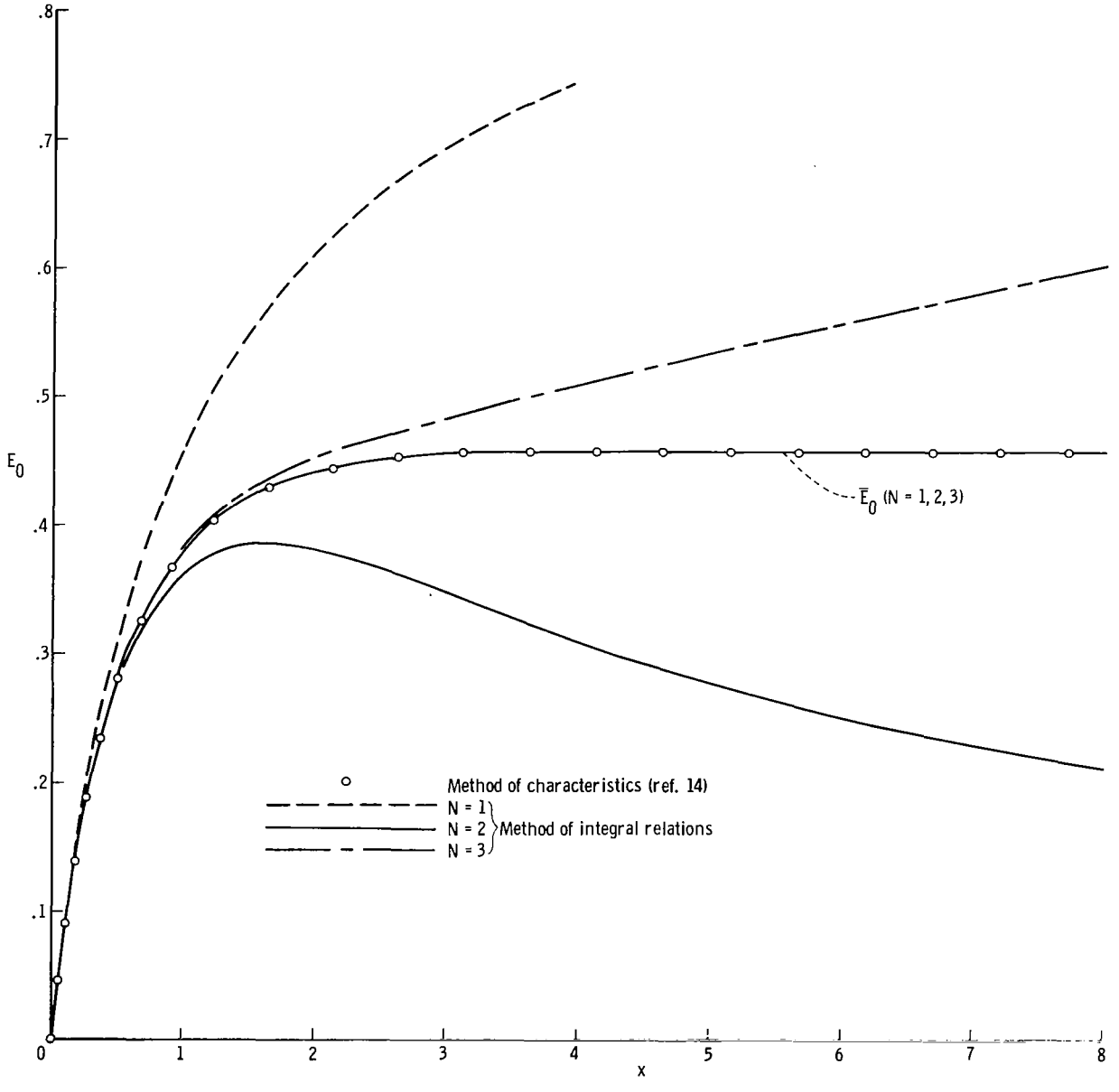

Figure 9.- Surface vibrational-energy distribution for a wedge. Case I.

occurred near the tip, regardless of the hyperbolic stability criterion used. It was found that if only the approximate differential equation for E_0 was discarded and replaced by equation (26), the solutions were stable, but the overall results were poor compared with those obtained by using the original approximate equations.

x,ψ Coordinates

It is known that the choice of dependent and independent variables is important in low approximations of the method of integral relations. If, for example, spherical polar coordinates are used for the cone solution (frozen or equilibrium flow), the results are less accurate for $N = 1$ than the corresponding results for the body-oriented x,y coordinates (see fig. 2 of ref. 13).

Since streamlines have a major role in nonequilibrium flows, the x,y coordinates were transformed to x,ψ coordinates, where ψ is the stream function. The integral relations were redeveloped for the wedge ($j = 0$) and $N = 2$. No particular advantage was evident since the strip boundaries are not streamlines, and there was no difference in the numerical results for case I obtained by use of either the x,ψ or the x,y coordinates.

Shock-Layer Profiles

Even in higher approximations, the details of the nonequilibrium flow between the shock wave and the body surface are not described accurately. At any downstream station x there are only $N + 1$ points along a normal to the surface from which flow-variable profiles can be obtained. Likewise, the poor asymptotic behavior, discussed previously, causes considerable error in the most interesting variable, T. In references 12 and 13 streamlines were used to obtain better details for $N = 1$.

Figure 10 illustrates the profiles of pressure and temperature obtained in reference 15 for case II at a station $x = 9.0$. The three points given by the integral method for $N = 2$ are also shown in the figure at a station $x = 8.0$ (the present calculations were not carried farther). Although the pressures agree reasonably well, the temperatures do not. The corrected surface temperature (ref. 13) $\bar{T}_0$ is shown to agree well with the characteristics result.

It appears that, if accurate details of the temperature and density profiles are required, additional calculations must be carried out along streamlines by using a procedure like that described in reference 13.

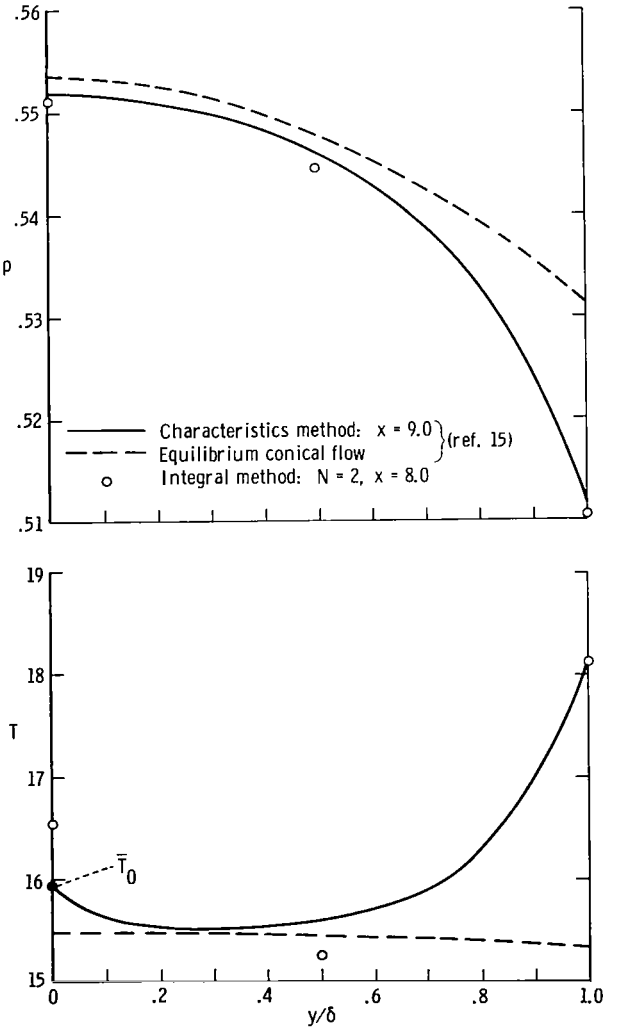

Figure 10.- Pressure and temperature profiles for a cone. Case II.

CONCLUDING REMARKS

The method of integral relations has been used to calculate supersonic, vibrationally relaxing flow past wedges and cones. Comparison of these calculations with characteristics calculations showed that the second, or two-strip, approximation was accurate for most of the approach to equilibrium. The asymptotic value of the surface vibrational energy did not converge to the correct value in higher approximations. The other flow variables were rather insensitive to this discrepancy, however, and the erroneous surface energy distribution was corrected.

For the present problem, in which the entire shock layer is supersonic, the original partial differential equations are of hyperbolic type. The approximate systems of ordinary differential equations correctly posed an initial-value problem. Control of the integration step size was necessary to achieve numerically stable solutions; the stability criterion is related to the hyperbolic characteristic curves.

It was found that the exact forms of the momentum and rate equations along the body surface could not be used in lieu of their counterparts in the approximate systems. Such a hybrid procedure always produced unstable numerical results near the wedge or cone tip.

Langley Research Center,
National Aeronautics and Space Administration,
Langley Station, Hampton, Va., June 4, 1964.

APPENDIX A

FROZEN SHOCK-WAVE RELATIONS

The appropriate frozen shock-wave relations are given for $\gamma = 7/5$ (ref. 18). Let

$$b(\beta, M_\infty) = M_\infty^2 \sin^2\beta \tag{A1}$$

$$a(\beta, M_\infty) = \frac{5}{6M_\infty^2}(b - 1) \tag{A2}$$

then

$$u(x,\delta) = u_\delta = (1 - a)\cos\theta + a \cot\beta \sin\theta \tag{A3}$$

$$v(x,\delta) = v_\delta = -(1 - a)\sin\theta + a \cot\beta \cos\theta \tag{A4}$$

$$p(x,\delta) = p_\delta = \frac{35b - 5}{42M_\infty^2} \tag{A5}$$

$$\rho(x,\delta) = \rho_\delta = \frac{6b}{5 + b} \tag{A6}$$

The β-derivatives of equations (A3) to (A6) are also required explicitly and they are, respectively,

$$\frac{du_\delta}{d\beta} = -\frac{5}{3}\cos\beta \sin\lambda - \frac{a \sin\theta}{\sin^2\beta} \tag{A7}$$

$$\frac{dv_\delta}{d\beta} = \frac{5}{3}\cos\beta \cos\lambda - \frac{a \cos\theta}{\sin^2\beta} \tag{A8}$$

$$\frac{dp_\delta}{d\beta} = \frac{5}{3}\sin\beta \cos\beta \tag{A9}$$

$$\frac{d\rho_\delta}{d\beta} = \frac{60b \cot\beta}{(5 + b)^2} \tag{A10}$$

APPENDIX B

COMPUTATIONAL EQUATIONS FOR N = 2

Before the final computational forms of the approximate systems are obtained, the derivatives of the functions $Q_{i,k}$ must be further expanded in terms of u_k, v_k, p_k, ρ_k, E_k, and $r_k{}^j$. The functions at the shock wave $Q_{i,\delta}$ are explicit functions of β (and r_δ when $j = 1$) so that $dQ_{i,\delta}/dx$ can be expressed in terms of the single derivative $d\beta/dx$ (and dr_δ/dx when $j = 1$). For example,

$$\frac{dQ_{3,\delta}}{dx} = r_\delta{}^j \frac{d}{dx}\left(\rho_\delta u_\delta v_\delta\right) + j\rho_\delta u_\delta v_\delta \frac{dr_\delta}{dx} \tag{B1a}$$

or

$$\frac{dQ_{3,\delta}}{dx} = (x \sin\theta + \delta\cos\theta)^j \frac{d}{d\beta}\left(\rho_\delta u_\delta v_\delta\right)\frac{d\beta}{dx} + j(\sin\theta + \tan\lambda\cos\theta)\rho_\delta u_\delta v_\delta \tag{B1b}$$

In any approximation the equation which contains $dQ_{3,0}/dx$ and $dQ_{3,\delta}/dx$ will yield the required expression for $d\beta/dx$ by using equations (B1b) and (11) and by noting that $Q_{3,0} = \rho_0 u_0 v_0 = 0$ for all values of x. Treating $d\beta/dx$ (and thus $dQ_{i,\delta}/dx$) as a known algebraic quantity effects considerable simplification, as follows: at each strip boundary the derivatives of the corresponding variables u_k, v_k, p_k, and E_k can be obtained by solution of a 4 by 4 linear algebraic system. (Eqs. (5) and (6) are used to eliminate derivatives of ρ_k.)

This feature is emphasized to point out that one does not have to deal directly with a $4N$ by $4N$ system but rather N (4 by 4) systems. The algebra required for the latter is simple, so that one need not resort to time-consuming inversion of a $4N$ by $4N$ matrix in the computer at each integration step.

The procedures are now demonstrated for $N = 2$. The derivatives of $r_k{}^j$ are expanded from the functions $Q_{i,k}$ ($k = 0,1,\delta$) as in equation (B1a), and then equations (18) are divided by $r_0{}^j$. Equations (18a) can be written (in the order $i = 3,1,2,4$)

$$\delta B_1 H_1 \frac{d\beta}{dx} = K_1 \tag{B2}$$

$$\delta \frac{d}{dx}\left(\rho_0 u_0\right) = K_2 \tag{B3}$$

$$\delta \frac{d}{dx}\left(p_0 + \rho_0 u_0^2\right) = K_3 \tag{B4}$$

$$\delta \frac{d}{dx}\left(\rho_0 u_0 E_0\right) = K_4 \tag{B5}$$

and equations (18b) can be written (in the order $i = 1,2,3,4$)

$$\delta B_2 \frac{d}{dx}\left(\rho_1 u_1\right) = K_5 \tag{B6}$$

$$\delta B_2 \frac{d}{dx}\left(p_1 + \rho_1 u_1^2\right) = K_6 \tag{B7}$$

$$\delta B_2 \frac{d}{dx}\left(\rho_1 u_1 v_1\right) = K_7 \tag{B8}$$

$$\delta B_2 \frac{d}{dx}\left(\rho_1 u_1 E_1\right) = K_8 \tag{B9}$$

where

$$K_1 = -2B_2\rho_1 u_1 v_1 \tan\lambda + \left(B_3 \tan\lambda - j\phi\right)\rho_\delta u_\delta v_\delta - 4\left[p_0 - B_2\left(p_1 + \rho_1 v_1^2\right) + B_1\left(p_\delta + \rho_\delta v_\delta^2\right)\right] - j\phi \cot\theta\left(p_0 - p_\delta\right) \tag{B10}$$

$$K_2 = \frac{H_2}{H_1} K_1 - (\tan\lambda + j\phi)\rho_0 u_0 + 2B_2\rho_1 u_1 \tan\lambda - \left(B_3 \tan\lambda - j\phi\right)\rho_\delta u_\delta - 4\left(B_2\rho_1 v_1 - B_1\rho_\delta v_\delta\right) \tag{B11}$$

$$K_3 = \frac{H_3}{H_1} K_1 - (\tan \lambda + j\phi)\left(p_0 + \rho_0 u_0^2\right) + 2B_2 \tan \lambda \left(p_1 + \rho_1 u_1^2\right)$$

$$- \left(B_3 \tan \lambda - j\phi\right)\left(p_\delta + \rho_\delta v_\delta^2\right) - 4\left(B_2 \rho_1 u_1 v_1 - B_1 \rho_\delta u_\delta v_\delta\right) + j\phi\left(p_0 - p_\delta\right) \tag{B12}$$

$$K_4 = -(\tan \lambda + j\phi)\rho_0 u_0 E_0 + 2B_2 \rho_1 u_1 E_1 \tan \lambda - 4B_2 \rho_1 v_1 E_1 + \delta\left(\rho_0 \epsilon_0 - B_1 \rho_\delta \epsilon_\delta\right) \tag{B13}$$

$$K_5 = - \frac{H_2}{H_1} K_1 - \left(B_4 \tan \lambda + 2j\phi\right)\rho_1 u_1 + \left(B_4 \tan \lambda - j\phi\right)\rho_\delta u_\delta + 2B_2 \rho_1 v_1 - 5B_1 \rho_\delta v_\delta \tag{B14}$$

$$K_6 = - \frac{H_3}{H_1} K_1 - \left(B_4 \tan \lambda + 2j\phi\right)\left(p_1 + \rho_1 u_1^2\right) + \left(B_4 \tan \lambda - j\phi\right)\left(p_\delta + \rho_\delta u_\delta^2\right)$$

$$+ 2B_2 \rho_1 u_1 v_1 - 5B_1 \rho_\delta u_\delta v_\delta + j\phi\left(2p_1 + p_\delta\right) \tag{B15}$$

$$K_7 = -K_1 - \left(B_4 \tan \lambda + 2j\phi\right)\rho_1 u_1 v_1 + \left(B_4 \tan \lambda - j\phi\right)\rho_\delta u_\delta v_\delta$$

$$+ p_0 + 2B_2\left(p_1 + \rho_1 v_1^2\right) - 5B_1\left(p_\delta + \rho_\delta v_\delta^2\right) + j\phi \cot \theta\left(2p_1 + p_\delta\right) \tag{B16}$$

$$K_8 = -\left(B_4 \tan \lambda + 2j\phi\right)\rho_1 u_1 E_1 + 2B_2 \rho_1 v_1 E_1 + \delta\left(B_2 \rho_1 \epsilon_1 + B_1 \rho_\delta \epsilon_\delta\right) \tag{B17}$$

$$\left.\begin{aligned} H_1 &= \frac{d}{d\beta}\left(\rho_\delta u_\delta v_\delta\right) \\ H_2 &= \frac{d}{d\beta}\left(\rho_\delta u_\delta\right) \\ H_3 &= \frac{d}{d\beta}\left(p_\delta + \rho_\delta u_\delta^2\right) \end{aligned}\right\} \tag{B18}$$

$$\left.\begin{aligned} B_1 &= 1 + j\phi \cot\theta \\ B_2 &= B_1 + 1 \\ B_3 &= 2B_1 + 1 \\ B_4 &= 3B_1 + 1 \end{aligned}\right\} \tag{B19}$$

The variable $\phi = \delta/x$ is introduced to maintain consistent numerical accuracy in the ratio δ/x near the cone tip.

The derivatives of $\rho_k u_k$ $(k = 0,1)$ are expanded by using equations (5) and (6) with $\gamma = 7/5$, as follows:

$$\frac{d}{dx}\left(\rho_k u_k\right) = \frac{1}{u_k}\left[1.4m_k^2 \frac{dp_k}{dx} + \left(1 + 0.4m_k^2\right)\rho_k u_k \frac{du_k}{dx} + 0.4m_k^2 \rho_k v_k \frac{dv_k}{dx} + \frac{\rho_k u_k^2}{T_k}\frac{dE_k}{dx}\right] \tag{B20}$$

where

$$m_k = u_k\left(\frac{1.4p_k}{\rho_k}\right)^{-1/2} \tag{B21}$$

Also,

$$\frac{d}{dx}\left(p_k + \rho_k u_k^2\right) = \frac{dp_k}{dx} + \rho_k u_k \frac{du_k}{dx} + u_k \frac{d}{dx}\left(\rho_k u_k\right) \tag{B22}$$

$$\frac{d}{dx}\left(\rho_k u_k v_k\right) = \rho_k u_k \frac{dv_k}{dx} + v_k \frac{d}{dx}\left(\rho_k u_k\right) \tag{B23}$$

$$\frac{d}{dx}\left(\rho_k u_k E_k\right) = \rho_k u_k \frac{dE_k}{dx} + E_k \frac{d}{dx}\left(\rho_k u_k\right) \tag{B24}$$

Equations (B20) to (B24) are substituted into equations (B3) to (B9) to arrive at the final equations which (together with eq. (B2)) complete the set for $N = 2$:

$$\delta B_1 H_1 \frac{d\beta}{dx} = K_1 \qquad (B2)$$

$$\delta \rho_0 u_0 \frac{dE_0}{dx} = K_4 - E_0 K_2 \qquad (B25)$$

$$\delta\left(m_0^2 - 1\right)\frac{dp_0}{dx} = -\left(1 + 1.4m_0^2\right)\left(K_3 - u_0 K_2\right) + u_0 K_2 - \delta \frac{\rho_0 u_0^2}{T_0}\frac{dE_0}{dx} \qquad (B26)$$

$$\rho_0 u_0 \frac{du_0}{dx} = -\frac{dp_0}{dx} + \frac{K_3 - u_0 K_2}{\delta} \qquad (B27)$$

$$\delta B_2 \rho_1 u_1 \frac{dE_1}{dx} = K_8 - E_1 K_5 \qquad (B28)$$

$$\delta B_2 \rho_1 u_1 \frac{dv_1}{dx} = K_7 - v_1 K_5 \qquad (B29)$$

$$\delta B_2\left(m_1^2 - 1\right)\frac{dp_1}{dx} = -\left(1 + 1.4m_1^2\right)\left(K_6 - u_1 K_5\right) + u_1 K_5 - 0.4\delta B_2 m_1^2 \rho_1 v_1 \frac{dv_1}{dx} - \delta B_2 \frac{\rho_1 u_1^2}{T_1}\frac{dE_1}{dx} \qquad (B30)$$

$$\rho_1 u_1 \frac{du_1}{dx} = -\frac{dp_1}{dx} + \frac{K_6 - u_1 K_5}{\delta} \qquad (B31)$$

$$\frac{d\phi}{dx} = \frac{1}{x}(\tan \lambda - \phi) \qquad (B32)$$

APPENDIX C

EXACT INITIAL DERIVATIVES FOR A WEDGE

Sedney (ref. 22) used natural coordinates to derive exact expressions for the shock curvature and the gradients of surface flow variables at the wedge tip caused by vibrational relaxation. A somewhat different approach, which is more appropriate to the present problem, yields an equivalent solution for $d\beta(0)/dx$ and the initial flow-variable gradients along any strip boundary.

The coordinates $\eta = y/\delta$ and $\xi = x$ are introduced to map the strips (fig. 2) into rectangular regions, with the shock at $\eta = 1$ and the surface at $\eta = 0$. In the $\xi\eta$-plane the wedge tip is the line $\xi = 0$, $0 \leq \eta \leq 1$. Derivatives of ρ are eliminated from equation (1) by using equations (4), (5), and (6); the transformed continuity, momentum, and vibrational-rate equations are as follows:

$$\delta\left(\frac{u}{\gamma p}\frac{\partial p}{\partial \xi} + \frac{\partial u}{\partial \xi}\right) + (v - u\eta \tan\lambda)\frac{1}{\gamma p}\frac{\partial p}{\partial \eta} - \eta \tan\lambda \frac{\partial u}{\partial \eta} + \frac{\partial v}{\partial \eta} = -\frac{\delta\epsilon}{T} \tag{C1}$$

$$\delta\left(u\frac{\partial u}{\partial \xi} + \frac{1}{\rho}\frac{\partial p}{\partial \xi}\right) + (v - u\eta \tan\lambda)\frac{\partial u}{\partial \eta} - \eta \frac{\tan\lambda}{\rho}\frac{\partial p}{\partial \eta} = 0 \tag{C2}$$

$$\delta u \frac{\partial v}{\partial \xi} + (v - u\eta \tan\lambda)\frac{\partial v}{\partial \eta} + \frac{1}{\rho}\frac{\partial p}{\partial \eta} = 0 \tag{C3}$$

$$\delta u \frac{\partial E}{\partial \xi} + (v - u\eta \tan\lambda)\frac{\partial E}{\partial \eta} = \delta\epsilon \tag{C4}$$

Equations (C1) to (C4) are differentiated again with respect to ξ, the limit as ξ and $\delta \to 0$ is obtained, and the following frozen-flow wedge conditions are applied:

$$\left.\begin{aligned} &v(0,\eta) = 0 \\ &\frac{\partial u}{\partial \eta}(0,\eta) = \frac{\partial v}{\partial \eta}(0,\eta) = \frac{\partial p}{\partial \eta}(0,\eta) = \frac{\partial E}{\partial \eta}(0,\eta) = 0 \end{aligned}\right\} \tag{C5}$$

Then at the wedge tip, that is, along the line $\xi = 0$,

$$\frac{u}{\gamma p}\left(P - \eta \frac{\partial P}{\partial \eta}\right) + \left(U - \eta \frac{\partial U}{\partial \eta}\right) + \cot \lambda \frac{\partial V}{\partial \eta} = - \frac{\epsilon}{\Pi} \tag{C6}$$

$$\rho u\left(U - \eta \frac{\partial U}{\partial \eta}\right) + P - \eta \frac{\partial P}{\partial \eta} = 0 \tag{C7}$$

$$\frac{\partial P}{\partial \eta} + \rho u \tan \lambda\left(V - \eta \frac{\partial V}{\partial \eta}\right) = 0 \tag{C8}$$

$$\Omega - \eta \frac{\partial \Omega}{\partial \eta} = \frac{\epsilon}{u} \tag{C9}$$

where

$$U = \frac{\partial u}{\partial \xi}(0,\eta)$$

$$V = \frac{\partial v}{\partial \xi}(0,\eta)$$

$$P = \frac{\partial p}{\partial \xi}(0,\eta)$$

$$\Omega = \frac{\partial E}{\partial \xi}(0,\eta)$$

The boundary conditions are as follows:

At $\eta = 1$,

$$\left.\begin{aligned} U(1) &= \frac{du_\delta}{d\beta}\frac{d\beta}{d\xi} \\ V(1) &= \frac{dv_\delta}{d\beta}\frac{d\beta}{d\xi} \\ P(1) &= \frac{dp_\delta}{d\beta}\frac{d\beta}{d\xi} \\ \Omega(1) &= 0 \end{aligned}\right\} \tag{C10a}$$

and at $\eta = 0$,

$$V(0) = 0 \tag{C10b}$$

The solution of equations (C6) to (C9) with the boundary conditions (C10) is readily obtained. In terms of the notation of the main text, the wedge initial derivatives at $x = 0$ are found to be

$$\frac{du_k}{dx} = \left[\eta_k \frac{du_\delta}{d\beta} - \frac{\left(1 - \eta_k\right)}{\rho_\delta u_\delta} \frac{dp_\delta}{d\beta}\right]\frac{d\beta}{dx} \tag{C11}$$

$$\frac{dv_k}{dx} = \eta_k \frac{dv_\delta}{d\beta} \frac{d\beta}{dx} \tag{C12}$$

$$\frac{dp_k}{dx} = \frac{dp_\delta}{d\beta} \frac{d\beta}{dx} \tag{C13}$$

$$\frac{dE_k}{dx} = \left(1 - \eta_k\right)\frac{\epsilon_\delta}{u_\delta} \tag{C14}$$

$$\frac{d\beta}{dx} = - \frac{\epsilon_\delta}{T_\delta}\left[\left(M_\delta{}^2 - 1\right)\frac{1}{\rho_\delta u_\delta} \frac{dp_\delta}{d\beta} + \cot \lambda \frac{dv_\delta}{d\beta}\right]^{-1} \tag{C15}$$

REFERENCES

1. Dorodnicyn, A. A.: A Contribution to the Solution of Mixed Problems of Transonic Aerodynamics. Vol. 2 of Advances in Aeronautical Sciences, Pergamon Press, 1959, pp. 832-844.

2. Chushkin, P. I. (J. W. Palmer, trans.): Calculation of Certain Sonic Flows of a Gas. Lib. Translation No.816, British R.A.E., Apr. 1959. (Available From ASTIA as AD 217902.)

3. Belotserkovskii, O. M.: Flow With a Detached Shock Wave About a Symmetrical Profile. Jour. Appl. Math. and Mech., vol. 22, no. 2, 1958, pp. 279-296.

4. Gold, Ruby, and Holt, Maurice: Calculation of Supersonic Flow Past a Flat-Headed Cylinder by Belotserkovskii's Method. Div. Appl. Math., Brown Univ. (AFOSR TN-59-199, AD 211-525), Mar. 1959.

5. Traugott, Stephen C.: An Approximate Solution of the Direct Supersonic Blunt-Body Problem for Arbitrary Axisymmetric Shapes. Jour. Aerospace Sci., vol. 27, no. 5, May 1960, pp. 361-370.

6. Holt, Maurice, and Hoffman, Gilbert H.: Calculation of Hypersonic Flow Past Spheres and Ellipsoids. [Preprint] 61-209-1903, American Rocket Soc., June 1961.

7. Holt, Maurice: Direct Calculation of Pressure Distribution on Blunt Hypersonic Nose Shapes With Sharp Corners. Jour. Aerospace Sci., vol. 28, no. 11, Nov. 1961, pp. 872-876.

8. Vaglio-Laurin, Roberto: On the PLK Method and the Supersonic Blunt-Body Problem. Jour. Aerospace Sci., vol. 29, no. 2, Feb. 1962, pp. 185-206, 248.

9. Traugott, Stephen C.: Some Features of Supersonic and Hypersonic Flow About Blunted Cones. Jour. Aerospace Sci., vol. 29, no. 4, Apr. 1962, pp. 389-399.

10. Chushkin, P. I., and Shchennikov, V. V. (B. A. Woods, trans.): Calculation of Certain Conical Flows Without Axial Symmetry. Lib. Translation No.926, British R.A.E., Dec. 1960.

11. Dorodnitsyn, A. A.: General Method of Integral Relations and Its Application to Boundary Layer Theory. Vol. 3 of Advances in Aeronautical Sciences, The Macmillan Co., 1962, pp. 207-219.

12. Shih, William C. L., Baron, Judson R., Krupp, Roy S., and Towle, William J.: Nonequilibrium Blunt Body Flow Using the Method of Integral Relations. Tech. Rep. 66 (Contract NOw 62-0765-d), Aerophys. Lab., M.I.T., May 1963. (Available From DDC as 415934.)

13. South, Jerry C., Jr.: Application of Dorodnitsyn's Integral Method to Nonequilibrium Flows Over Pointed Bodies. NASA TN D-1942, 1963.

14. Sedney, R., South, J. C., and Gerber, N.: Characteristic Calculation of Non-Equilibrium Flows. Rep. No. 1173, Ballistic Res. Labs., Aberdeen Proving Ground, Apr. 1962.

15. Sedney, R., and Gerber, N.: Nonequilibrium Flow Over a Cone. Rep. No. 1203, Ballistic Res. Labs., Aberdeen Proving Ground, May 1963.

16. Bobbitt, Percy J.: Effects of Shape on Total Radiative and Convective Heat Inputs at Hyperbolic Entry Speeds. Advances in Astronautical Sci., vol. 13, Eric Burgess, ed., Western Periodicals Co. (N. Hollywood, Calif.), c.1963, pp. 290-319.

17. Allen, H. Julian: Gas Dynamics Problems of Space Vehicles. Proceedings of the NASA-University Conference on the Science and Technology of Space Exploration, Vol. 2, NASA SP-11, 1962, pp. 251-267. (Also available as NASA SP-24.)

18. Ames Research Staff: Equations, Tables, and Charts for Compressible Flow. NACA Rep. 1135, 1953. (Supersedes NACA TN 1428.)

19. Newman, Perry A.: Approximate Calculation of Hypersonic Conical Flow Parameters for Air in Thermodynamic Equilibrium. NASA TN D-2058, 1964.

20. Romig, Mary F.: Conical Flow Parameters for Air in Dissociation Equilibrium. Res. Rep. No. 7, Convair Sci. Res. Lab., May 15, 1960. (Supersedes Res. Note 14.)

21. Ferri, Antonio: Supersonic Flows With Shock Waves. General Theory of High Speed Aerodynamics. Vol. VI of High Speed Aerodynamics and Jet Propulsion, sec. H, W. R. Sears, ed., Princeton Univ. Press, 1954, pp. 670-747.

22. Sedney, Raymond: Some Aspects of Nonequilibrium Flows. Jour. Aerospace Sci., vol. 28, no. 3, Mar. 1961, pp. 189-196, 208.

NASA-Langley, 1964 L-3974